Ezetimibe blocks the internalization of NPC1L1 and cholesterol in mouse small intestine

Chang Xie (谢畅),[1] **Zhang-Sen Zhou (周章森),**[1] **Na Li (李钠), Yan Bian (卞艳),**
Yong-Jian Wang (王永建), Li-Juan Wang (王丽娟), Bo-Liang Li (李伯良),[2]
and Bao-Liang Song (宋保亮)[2]

The State Key Laboratory of Molecular Biology, Institute of Biochemistry and Cell Biology, Shanghai
Institutes for Biological Sciences, Chinese Academy of Sciences, Shanghai 200031, China

Abstract The multiple transmembrane protein Niemann-Pick C1 like1 (NPC1L1) is essential for intestinal cholesterol absorption. Ezetimibe binds to NPC1L1 and is a clinically used cholesterol absorption inhibitor. Recent studies in cultured cells have shown that NPC1L1 mediates cholesterol uptake through vesicular endocytosis that can be blocked by ezetimibe. However, how NPC1L1 and ezetimibe work in the small intestine is unknown. In this study, we found that NPC1L1 distributed in enterocytes of villi and transit-amplifying cells of crypts. Acyl-CoA cholesterol acyltransferase 2 (ACAT2), another important protein for cholesterol absorption by providing cholesteryl esters to chylomicrons, was mainly presented in the apical cytoplasm of enterocytes. NPC1L1 and ACAT2 were highly expressed in jejunum and ileum. ACAT1 presented in the Paneth cells of crypts and mesenchymal cells of villi. In the absence of cholesterol, NPC1L1 was localized on the brush border of enterocytes. Dietary cholesterol induced the internalization of NPC1L1 to the subapical layer beneath the brush border and became partially colocalized with the endosome marker Rab11. Ezetimibe blocked the internalization of NPC1L1 and cholesterol and caused their retention in the plasma membrane.■ This study demonstrates that NPC1L1 mediates cholesterol entering enterocytes through vesicular endocytosis and that ezetimibe blocks this step in vivo.—Xie, C., Z-S. Zhou, N. Li, Y. Bian, Y-J. Wang, L-J. Wang, B-L. Li, and B-L. Song. **Ezetimibe blocks the internalization of NPC1L1 and cholesterol in mouse small intestine.** *J. Lipid Res.* 2012. 53: 2092–2101.

Supplementary key words Niemann-Pick C1 like1 • cholesterol absorption • endocytosis • transport

Dietary cholesterol absorption in small intestine is a major way for mammals to obtain cholesterol. In intestinal lumen, cholesterol incorporates into bile salt micelles and diffuses to the brush border membrane of enterocytes (1). Then cholesterol moves to the endoplasmic reticulum (ER) and is esterified by ACAT2 (1–5). Finally, the newly formed cholesterol ester is packed into chylomicrons and secreted to lymph (1).

The Niemann-Pick C1 like1 (NPC1L1) protein is the gatekeeper of dietary cholesterol absorption. Genetic deletion of *NPC1L1* decreases cholesterol absorption by more than 70% in mice (6). In rodents, NPC1L1 is selectively expressed in the small intestine and localizes on the brush border membrane (6–8). It has been proposed that NPC1L1 mediates cholesterol movement into enterocytes in vivo. However, direct evidence is lacking.

Studies in cultured cells indicate that NPC1L1 facilitates cholesterol entering cytoplasm by vesicular endocytosis (9, 10). NPC1L1 forms cholesterol-enriched membrane microdomains on plasma membrane with lipid raft proteins Flotillin-1/-2 (11). The NPC1L1-Flotillin-cholesterol microdomains are internalized via clathrin/AP2 pathway and transported to the endocytic recycling compartment (ERC) (9, 11). The ERC is a cellular cholesterol pool and a Rab11a-positive compartment (9, 12–14). When the ERC cholesterol level drops, NPC1L1 moves to plasma membrane to mediate another round of cholesterol transport (9, 13, 15–17). Ezetimibe, a cholesterol absorption inhibitor, blocks the internalization of NPC1L1-Flotillin-cholesterol microdomains and therefore decreases cholesterol uptake in cultured cells (9, 11, 17, 18). How NPC1L1 and ezetimibe work in vivo is unknown.

There are two isoforms of ACAT enzymes in mammals, the ACAT1 and ACAT2. ACAT1 is ubiquitously expressed in all tissues, whereas ACAT2 is specifically expressed in liver and small intestine (19–24). Previous studies have indicated

Abbreviations: ACAT, acyl-CoA cholesterol acyltransferase; ER, endoplasmic reticulum; ERC, endocytic recycling compartment; MTP, microsomal triglyceride transfer protein; NPC1L1, Niemann-Pick C1 like1.
[1] These authors contribute equally to this work.
[2] To whom correspondence should be addressed.
  e-mail: blli@sibs.ac.cn; blsong@sibs.ac.cn

that the major ACAT activity in small intestine is ACAT2 (4, 20, 22). ACAT2 is essential for efficient intestinal cholesterol absorption (2, 4, 25).

We studied the process of intestinal cholesterol absorption in vivo. The specific antibodies were raised to detect mouse endogenous NPC1L1, ACAT1, and ACAT2. Immunohistological staining revealed that NPC1L1 localized to the brush border of enterocytes and that ACAT2 mainly localized to the ER of enterocytes. ACAT1 was barely detected in enterocytes and was enriched in Paneth cells and mesenchymal cells. Cholesterol administration induced the endocytosis of NPC1L1, which partially colocalized with Rab11 at the subapical sites beneath the brush border. Moreover, ezetimibe treatment inhibited the internalization of NPC1L1 and cholesterol, rendering their retention on brush boarder.

MATERIALS AND METHODS

Animals

C57BL/6 mice were from Shanghai SLAC Laboratory Animal Co., Ltd. (Shanghai, China). *ACAT1* (B6.129S4-*Soat1*[tm1Far]/J) and *ACAT2* (B6.129S4-*Soat2*[tm1Far]/J) heterozygous knockout mice were from Jackson Laboratory (Bar Harbor, ME) and crossed with C57BL/6 mice continually to obtain a uniform genetic background. The homozygous knockout mice ($ACAT1^{-/-}$ and $ACAT2^{-/-}$) were then generated by intercrossing heterozygous mice (4, 26). All mice were fed on a chow diet ad libitum and housed in a pathogen-free animal facility in plastic cages at 22°C, with a daylight cycle from 06:00 to 18:00. All animal procedures were approved by the Institutional Animal Care and Use Committee.

Antibodies

Goat polyclonal anti-villin and anti-lysozyme, rabbit polyclonal anti-mucin2 and anti-chromogranin A were from Santa Cruz Biotechnology (Santa Cruz, CA). Rabbit anti-Ki67 was from Bethyl Laboratories (Montgomery, TX). Mouse monoclonal anti-Rab11 antibody was from BD Transduction Laboratories™ (Franklin Lakes, NJ). Alexa Fluor 555 conjugated donkey anti-rabbit, Alexa Fluor 488 conjugated donkey anti-goat, and Alexa Fluor 488-conjugated goat anti-mouse secondary antibodies were from Invitrogen (Camarillo, CA). HRP-conjugated donkey anti-goat secondary antibody was from Santa Cruz Biotechnology. HRP-conjugated goat anti-mouse and donkey anti-rabbit secondary antibodies were from Thermo Fisher Scientific Inc. (Rockford, IL).

Generation of anti-NPC1L1, ACAT1, and ACAT2 polyclonal antibodies

Rabbit polyclonal anti-mouse NPC1L1 antibody was raised in rabbits immunized with 6×His fused C-terminal 67 amino acids of mouse origin. Rabbit polyclonal anti-mouse ACAT1 and ACAT2 antibodies were raised in rabbits immunized with 6×His fused N-terminal amino acids 1–103 of ACAT1 and 8–91 of ACAT2, respectively. Antisera were affinity purified with glutathione S-transferase-fused antigens. Affinity-purified anti-NPC1L1 antibody was dialyzed in PBS and concentrated by ultrafiltration before being labeled with Alexa Fluor 488 according to the user manual (Invitrogen).

Cholesterol feeding and ezetimibe treatment

For cholesterol feeding, 12-week-old male C57BL/6 mice (n = 6 per group) were gavaged with 200 µl corn oil containing 40 mg/ml cholesterol. After 30 min, the mice were euthanized, and the intestines were taken and subjected to various analyses.

For ezetimibe treatment, 12-week-old male C57BL/6 mice (n = 6 per group) were pretreated with ezetimibe (10 mg/kg/day) or vehicle by oral gavage once daily for 3 days (6). On day 4, the mice were gavaged with ezetimibe (10 mg/kg/day) or vehicle. After 30 min, the mice were gavaged with 150 µl corn oil containing 40 mg/ml cholesterol. After an additional 30 min, the mice were euthanized, and the intestines were taken. The duodenum, jejunum, and ileum were isolated as previously described (27). The middle 3-cm part of the duodenum, jejunum, ileum, and colon were taken, of which the first 1-cm fragment was used for lipid extraction and the rest was applied to filipin staining and immunohistochemical staining.

Immunohistochemistry

Intestinal tissues were washed in PBS and fixed in 4% paraformaldehyde for 4 h at 4°C before preparation of 4-µm paraffin sections. Before antibody staining, the sections were deparaffinized in xylene and rehydrated in gradient ethanol and then subjected to high-temperature antigen retrieval in 50 mM Tris-HCl (pH 9.0) and 1 mM EDTA. Sections were blocked and permeabilized in PBS plus 0.5% Triton X-100 and 5% FBS (28). Primary antibodies of different species were incubated together in the staining procedure. For costaining with primary antibodies of the same species, such as rabbit anti-NPC1L1 and rabbit anti-Mucin2, anti-Ki67 or anti-ACAT2, unlabeled primary antibody (anti-Mucin2, anti-Ki67 or anti-ACAT2), and Alexa Fluor 555-conjugated donkey anti-rabbit secondary antibody were sequentially added, and then sections were washed and blocked with rabbit IgG for 30 min before incubation with Alexa Fluor 488-labeled rabbit anti-NPC1L1 antibody. After immunoreaction, sections were incubated with Hoechst for 5 min before mounting. Slides were detected under Leica SP5 microscopy.

Filipin staining

Intestinal tissues were washed in PBS and fixed in 4% paraformaldehyde for 4 h at 4°C and dehydrated in 30% sucrose overnight at 4°C before being embedded in tissue-freezing medium (Leica Microsystems, Buffalo Grove, IL). Frozen sections (8 µm) were prepared with a Leica CM 3050S cryostat. The frozen sections were washed in PBS and stained with filipin (50 µg/ml in PBS plus 10% FBS) for 30 min at room temperature, washed with PBS, and mounted (29).

Cholesterol absorption assay

The fecal dual isotope ratio method was applied to measure cholesterol absorption in mice (30, 31). Briefly, 12-week-old male C57BL/6 mice (n = 6 per group) were pretreated with ezetimibe (10 mg/kg/day) or vehicle for 3 days as described above. On day 4, the mice were gavaged with ezetimibe (10 mg/kg/day) or vehicle. After 30 min, the mice were further gavaged with 150 µl corn oil containing [14C]-cholesterol (0.5 µCi), [3H]-sitosterol (1 µCi), and 0.1 mg unlabeled cholesterol. Feces were collected daily for 3 days, and [14C]-cholesterol and 3H-sitosterol were determined to calculate the cholesterol absorption. The percent cholesterol absorption was calculated as follows: % cholesterol absorption = $([^{14}C]/[^{3}H]$ dosing mixture $- [^{14}C]/[^{3}H]$ feces$)/([^{14}C]/[^{3}H]$ dosing mixture$) \times 100$.

Western blot

Mouse tissues were removed, quickly washed with ice-cold PBS, and homogenized in RIPA buffer (50 mM Tris-HCl [pH 8.0], 150 mM NaCl, 2 mM $MgCl_2$, 0.1% SDS, 1.5% Nonidet P-40, 0.5% deoxycholate) with protease inhibitors (1% protease inhibitor

cocktail [P8340; Sigma, St. Louis, MO] plus 5 µg/ml pepstatin A, 10 µg/ml leupeptin, 10 µM MG-132, 1 mM PMSF, and 25 µg/ml ALLN), and centrifuged at 13,200 rpm for 10 min. The supernatant was mixed 1:1 with membrane protein solubilization buffer (62.5 mM Tris-HCl [pH 6.8], 15% SDS, 8 M urea, 100 mM dithiothreitol) and then mixed with 4× loading buffer (150 mM Tris-HCl [pH 6.8], 12% SDS, 6% β-mecaptoethanol, 30% glycerol, 0.032% bromophenol blue) (32). From each sample, 50 µg of total protein was subjected to SDS-PAGE and analyzed by Western blotting.

PNGase F digestion

Protein glycosylation assay was carried out as previously described (33). Briefly, 63 µl homogenates of mouse small intestine in RIPA buffer were to with 7 µl 10× glycoprotein denaturing buffer (5% SDS, 0.4 M dithiothreitol) and incubated at 100°C for 10 min. After the addition of 9 µl 10% Nonidet P-40 and 9 µl G7 buffer, 2 µl PNGase F (New England Biolabs, Ipswich, MA) or vehicle buffer were added, and the mixture was incubated at 37°C for 1 h. Then the membrane protein solubilizing buffer and

4× loading buffer were sequentially added into the mixture. Reaction products were separated via SDS-PAGE and analyzed by Western blotting.

Real-time quantitative PCR

Intestinal tissues were excised and washed quickly before homogenized in Tri reagent (T9424; Sigma, St. Louis, MO). From each sample, 2 µg RNA was reverse transcribed to obtain the cDNA template for real-time quantitative PCR amplification. Real-time amplification was achieved with SsoFast™ EvaGreen supermix with low ROX (Bio-Rad, Hercules, CA) using a Stratagene MX3005P QPCR system (La Jolla, CA). The relative amount of mRNA was normalized to that of *Cyclophilin* (34). The relative amount of mRNA in colon was set to a normalized value of 1 unit. The primers for mouse *NPC1L1* were 5′-TTGCCTTGACCTC-TGGCTTAG-3′ and 5′-AGGGCGGATGAATCTGTGC-3′. The primers for mouse *ACAT1* were 5′-CCGAGACAACTACCCAAGGA-3′ and 5′-CACACACAGGACCAGGACAC-3′. The primers for mouse *ACAT2* were 5′-ATGTTCTACCGGGACTGGTG-3′ and 5′-CCCG-AAAACAAGGAATAGCA-3′.
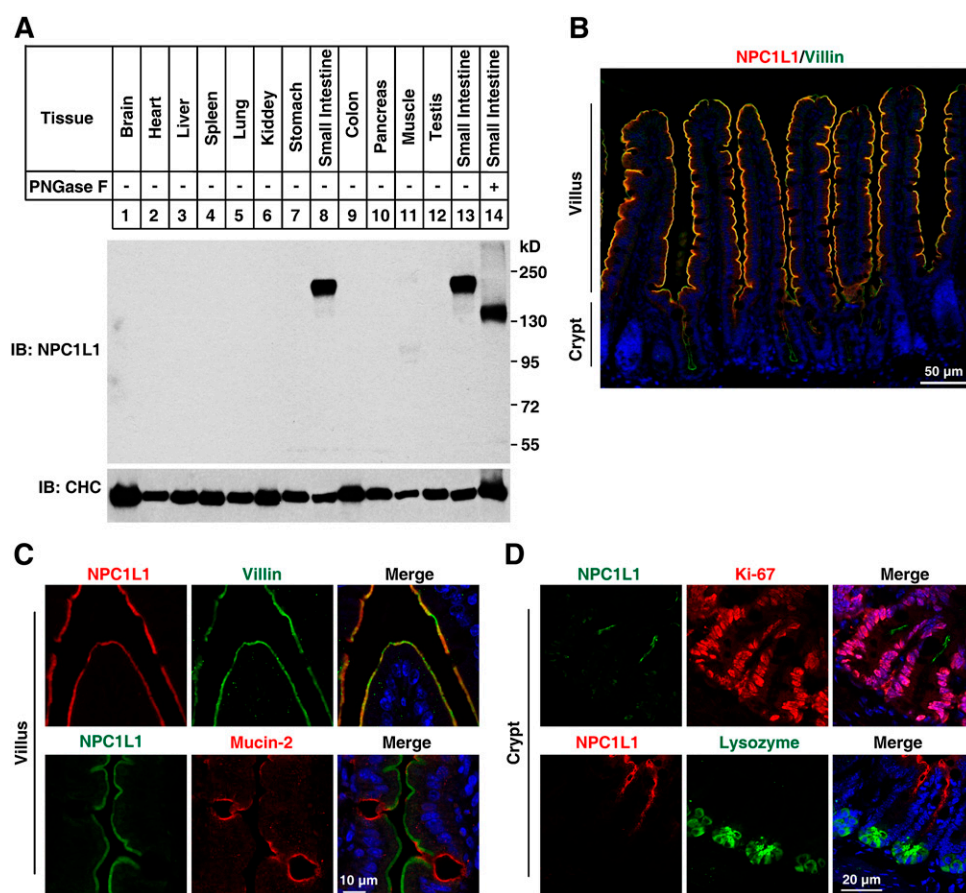

Fig. 1. Expression profile and localization of mouse NPC1L1. A: NPC1L1 is specifically expressed in mouse small intestine. Tissues taken from C57BL/6 mice were immediately homogenized. From each sample, 50 µg of total protein was loaded in SDS-PAGE and immunoblotted with the affinity-purified rabbit anti-NPC1L1 polyclonal antibody. For glycosylation analysis, homogenates of small intestine were subjected to PNGase F digestion. B: NPC1L1 protein mainly distributes in the villi of mouse small intestine. Intestinal sections (4 µm) were deparaffinized and stained with anti-NPC1L1 and anti-Villin (microvilli) antibodies. Scale bar: 50 µm. C: Enlarged view of the villi tips, showing that NPC1L1 localizes at the apical membrane of enterocytes. Small intestinal samples were costained with anti-NPC1L1 and anti-Villin (absorptive enterocytes) or anti-Mucin2 (goblet cells) antibodies. Scale bar: 10 µm. D: Enlarged view of the crypts showing that NPC1L1 also expresses in the transit-amplifying cells. Small intestinal samples were costained with anti-NPC1L1 and anti-Ki67 (proliferating cells) or anti-Lysozyme (Paneth cells) antibodies. The color of the title matches the stain color in the photomicrographs. Nuclear counterstaining with Hoechst is blue. Scale bar: 20 µm.

Measurement of intestinal lipids

Intestinal tissues (1 cm) taken from the same location of different groups were washed thoroughly with PBS and homogenized in 1 ml chloroform/methanol (2:1), vortexed for 1 h, mixed with 200 µl Milli-Q water, and centrifuged at 2,000 g for 10 min, and then 50 µl of organic phase was freeze-dried and applied to measure total cholesterol and phospholipids with enzymatic kits (35).

RESULTS

Murine NPC1L1 is specifically expressed in the villi and crypts of small intestine

To gain insight into the expression prolife of NPC1L1 in mice tissues, we raised a polyclonal antibody (pAb) against NPC1L1. Immunoblotting of tissue homogenates with the NPC1L1 pAb revealed a strong signal at 180 kDa in the small intestine (**Fig. 1A**), slightly larger than the predicted molecular weight of 146 kDa. However, the NPC1L1 protein was not detectable in brain, heart, liver, spleen,

lung, kidney, stomach, colon, pancreas, muscle, and testis (Fig. 1A). Because NPC1L1 contains multiple potential N-glycosylation sites and because protein glycosylation is essential for its function, we analyzed this modification with small intestin tissues. The NPC1L1 protein migrated faster (Fig. 1A, lanes 13 and 14) after PNGase F treatment, indicating that it was glycosylated in vivo (Fig. 1A).

Immunostaining of paraffin-embedded mouse small intestinal samples with anti-NPC1L1 and anti-Villin (labels the microvilli) antibodies were performed to investigate the vertical distribution of NPC1L1. The well colocalization of NPC1L1 and Villin showed that NPC1L1 was enriched in brush border membrane of the small intestine (Fig. 1B).

Enlarged images were taken to show the precise localization of NPC1L1 in villi and crypts. In epithelial enterocytes, NPC1L1 colocalized with Villin but not Mucin2, a marker for goblet cells (Fig. 1C), indicating that NPC1L1 localized in the brush border membrane of absorptive enterocytes. NPC1L1 was also detected in the crypts. The
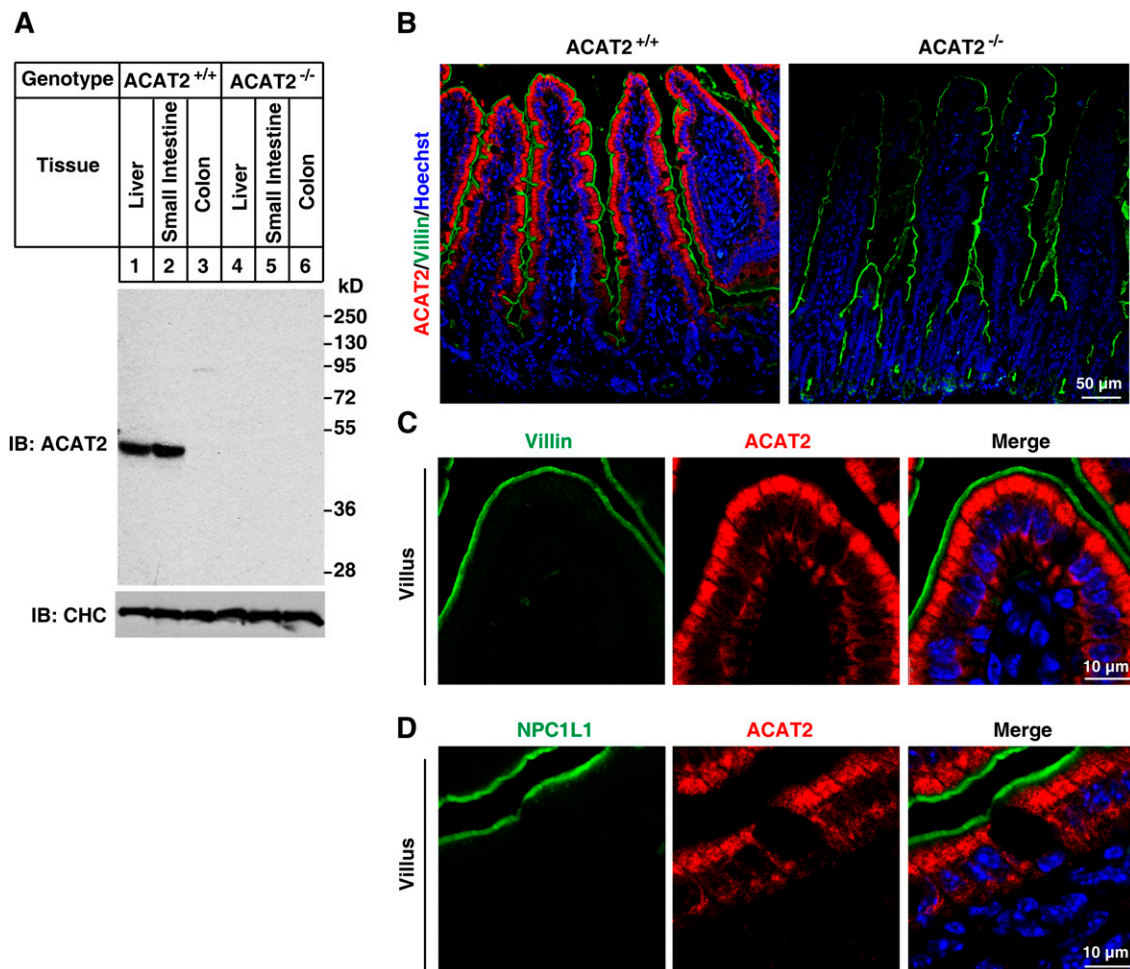

Fig. 2. Localization of ACAT2 in mouse small intestine. A, B: Validation of the affinity-purified anti-ACAT2 antibody. Liver, small intestine, and colon samples from *ACAT2*^{+/+} and *ACAT2*^{−/−} mice were homogenized and subjected to SDS-PAGE followed by immunoblotting with affinity-purified rabbit anti-ACAT2 polyclonal antibody (A). Deparaffinized 4-µm sections of small intestine sample from *ACAT2*^{+/+} and *ACAT2*^{−/−} mice were stained with anti-ACAT2 and anti-Villin antibodies (B). C, D: Enlarged view of the villi tips showing that NPC1L1 and ACAT2 localize to the different regions of intestinal epithelium. Intestinal samples were costained with purified anti-ACAT2 and anti-Villin (C) or anti-NPC1L1 (D) antibodies.
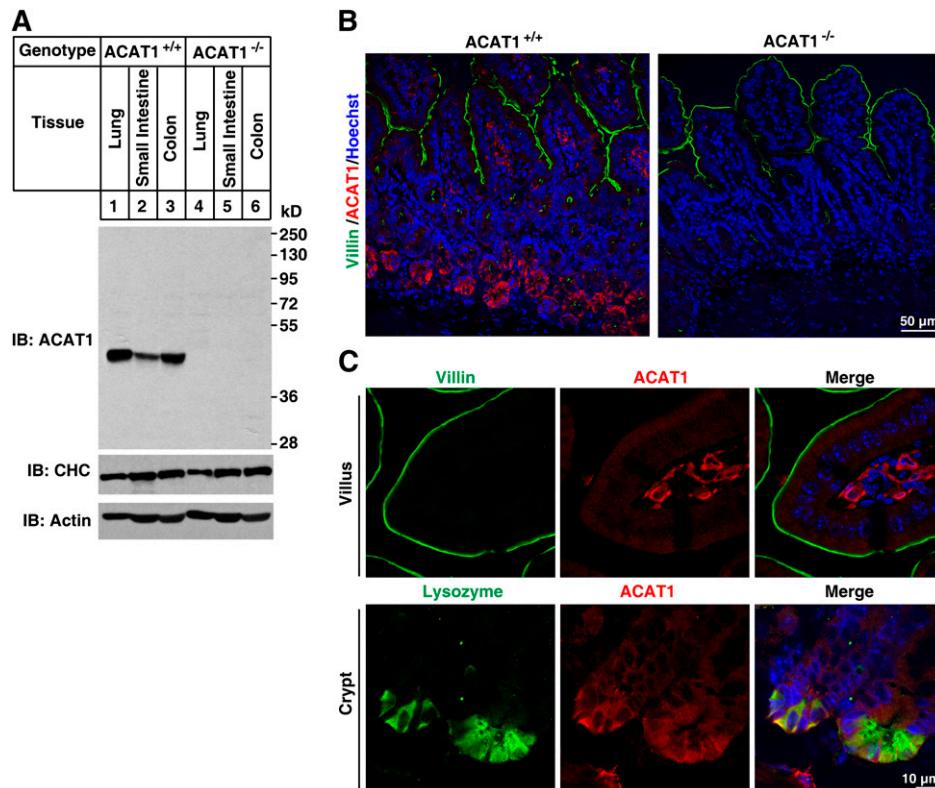
Fig. 3. Localization of ACAT1 in mouse small intestine. A, B: Validation of purified anti-ACAT1 antibody. Lung, small intestine, and colon samples from $ACAT1^{+/+}$ and $ACAT1^{-/-}$ mice were homogenized and subjected to SDS-PAGE followed by immunoblotting with the affinity-purified rabbit anti-ACAT1 polyclonal antibody (A). Deparaffinized 4-μm sections of small intestine samples from $ACAT1^{+/+}$ and $ACAT1^{-/-}$ mice were stained with anti-ACAT1 and anti-Villin antibodies (B). C: ACAT1 localized to mesenchymal cells of the villi and Paneth cells of the crypts. Paraffin-embedded intestinal sections were costained with anti-ACAT1 and anti-Villin or anti-Lysozyme antibodies, respectively.

intestinal crypts consist of stem cells, Paneth cells, and transit-amplifying cells. Stem cells and Paneth cells intersperse each other in the bottom, whereas transit-amplifying cells localize to the upper part of the crypts (36). To further elucidate which kind of cells NPC1L1 localized in the crypts, Ki67 and lysozyme were used as markers for proliferating cells (including stem cells and transit-amplifying cells) and Paneth cells, respectively. NPC1L1 was present in the apical sites of transit-amplifying cells that locate to the upper region of crypts but was absent in lysozyme-positive bottom cells (Fig. 1D).

Together, these data indicated that NPC1L1 is exclusively expressed in small intestine. It presents in the enterocytes and transit-amplifying cells in mouse small intestine and is preferentially located in the apical membrane.

ACAT2 is specifically expressed in absorptive enterocytes, whereas ACAT1 is enriched in Paneth cells of the crypts and mesenchymal cells of the villi

After entering enterocytes, cholesterol is esterified to cholesterol ester on ER by ACAT enzymes, which consists of two isoforms (ACAT1 and ACAT2) in mammals. ACAT1 and ACAT2 bear about 57% identities at the C terminus but show no similarities at the N-terminus (37–40). To explore the localization of ACATs in mouse small intestine, polyclonal anti-ACAT1 and anti-ACAT2 antibodies were

raised and purified. Then, we validated the antibodies by immunoblotting analysis with $ACAT1^{-/-}$ or $ACAT2^{-/-}$ mice tissues.

ACAT2 is selectively expressed in liver and small intestine but not in colon (**Fig. 2A**). In contrast, ACAT1 is ubiquitously expressed (**Fig. 3A**). These antibodies are of high specificity because no cross-reactive bands and no signal in tissues of $ACAT1^{-/-}$ (Fig. 3A) and $ACAT2^{-/-}$ (Fig. 2A) mice were detected.

The immunostaining of small intestine sections showed that ACAT2 was specifically expressed in epithelial enterocytes (the Villin-positive cells) (Fig. 2B, C). Magnified images further indicated that ACAT2 localized to the cytoplasm of enterocytes (mainly in the apical part) but had no colocalization with NPC1L1 or Villin (Fig. 2C, D). In contrast, ACAT1 was abundant in Paneth cells of the crypts and mesenchymal cells of the villi but was barely detected in other cells of the intestinal epithelial layer (Fig. 3B, C). These distribution data indicate that the major ACAT enzyme for cholesterol esterification in enterocytes is ACAT2.

Longitudinal expression of NPC1L1, ACAT1, and ACAT2 in mouse intestine

We compared the protein and mRNA levels of NPC1L1, ACAT1, and ACAT2 among different segments of mouse
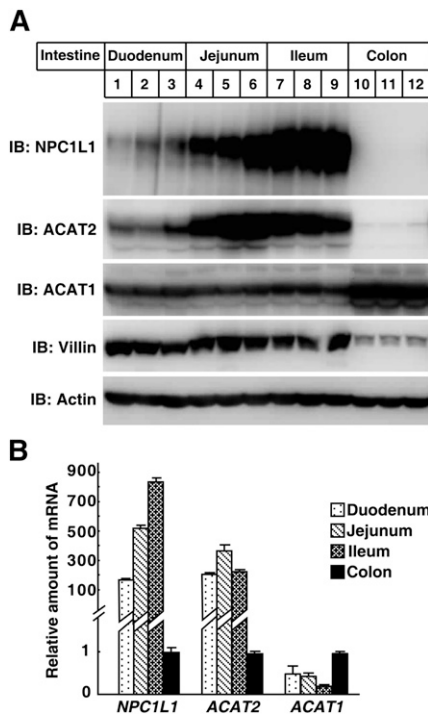
Fig. 4. Distribution of NPC1L1, ACAT1, and ACAT2 in mouse intestine. A: Immunoblot analysis of NPC1L1, ACAT1, and ACAT2 in mouse duodenum, jejunum, ileum, and colon. Immunoblots were performed with tissue homogenates using the purified polyclonal anti-NPC1L1, ACAT1, and ACAT2 antibodies. Three mice were used per segment. B: Quantitative PCR analysis of the gene expression of *NPC1L1*, *ACAT1*, and *ACAT2* in mouse duodenum, jejunum, ileum, and colon. The expression level of cyclophilin was used as an internal control. The relative amounts of mRNA in different segments of intestine were normalized with relative amounts of mRNA in colon. Values are mean ± SD.

intestine. The samples of middle duodenum, jejunum, ileum, and colon from three C57BL/6 adult mice were subjected to Western blot and quantitative PCR analysis. The protein level of NPC1L1 was relatively lower in duodenum and higher in jejunum and ileum but absent in colon (**Fig. 4A**). In addition, quantitative PCR analysis showed that the *NPC1L1* mRNA in small intestine was at least 100-fold of that in colon. The ACAT2 protein and mRNA expression pattern was similar to NPC1L1 (Fig. 4A, B); however, ACAT1 was expressed in all these segments, but the expression level was higher in colon than in the small intestine (Fig. 4A, B). Taken together, these observations show that the expression pattern of NPC1L1 and ACAT2, not ACAT1, is similar throughout the mouse small intestine.

Dietary cholesterol induces the endocytosis of NPC1L1 from brush border membrane

Previous studies have shown that cholesterol replenishment induces the endocytosis of NPC1L1 together with cholesterol from the plasma membrane to the ERC in cultured cells (9). To elucidate the physiological regulation of NPC1L1 in vivo, we analyzed its translocation in mouse small intestine. The mice were gavaged with or without cholesterol, and the intestinal tissues were collected to analyze the localization of NPC1L1. In the absence of

cholesterol, NPC1L1 localized mainly to brush border membrane and well colocalized with Villin, but not Rab11, in chow diet- (data not shown) or corn oil-gavaged mice (**Fig. 5A**, upper panels). However, when the mice were gavaged with cholesterol, substantial amounts of NPC1L1-positive vesicles were found just beneath the Villin-positive membrane and partially colocalized with Rab11, a marker of recycling endosomes (Fig. 5A, bottom panels). There was no obvious colocalization between NPC1L1 and ACAT2 under these conditions, suggesting that the transport of cholesterol from NPC1L1-positive compartments to ER is necessary.

To visualize the distribution of cholesterol, we used filipin to stain free cholesterol in the intestine. In the corn oil-gavaged mice, the cholesterol signal was very weak and mainly present on the brush boarder. However, the cholesterol staining became much stronger in the mouse intestine gavaged with cholesterol (Fig. 5B). Cholesterol distributed throughout the cells except in the nuclei. The cholesterol signal in apical cytoplasm was stronger than that in the basal part (Fig. 5B). We also used the enzymatic method to measure cholesterol level of intestinal epithelial cells. Compared with corn oil-gavaged mice, the whole intestinal cholesterol level increased by about 70% in the mice receiving cholesterol (Fig. 5C).

Together, these data demonstrate that NPC1L1 was transported from the brush border to the recycling endosomes during cholesterol absorption in mouse small intestine (Fig. 5A).

Ezetimibe blocks the internalization of NPC1L1 and cholesterol in intestinal enterocytes

Ezetimibe is a specific inhibitor of NPC1L1 and efficiently inhibits cholesterol absorption (6, 41). Previous studies in cultured cells have revealed that ezetimibe blocked the uptake of cholesterol by inhibiting the endocytosis of NPC1L1 (9, 18). Whether the cholesterol-induced endocytosis of NPC1L1 in enterocytes could be blocked by ezetimibe was further investigated. In cholesterol-gavaged mice without ezetimibe treatment, endocytic NPC1L1 was transported to the layer beneath the brush border. These NPC1L1 vesicles also showed partial colocalization with Rab11, implying that they were recruited in recycling compartments (**Fig. 6A**, upper panels). In the mice treated with ezetimibe, no obvious NPC1L1 vesicles were observed under the brush border (Fig. 6A, lower panels), demonstrating that the endocytosis of NPC1L1 was blocked by ezetimibe.

To ascertain whether cholesterol entered enterocytes when treated by ezetimibe, filipin staining of intestinal sections was performed. The no-ezetimibe treatment samples exhibited intracellular accumulated free cholesterol (Fig. 6B). However, the samples from ezetimibe-treated mice showed that free cholesterol remained at the brush border and that intracellular cholesterol was very low (Fig. 6B, left). An enzymatic measurement of total cholesterol and phospholipids of intestinal epithelial cells also showed that the cholesterol level was significantly decreased with ezetimibe treatment (Fig. 6C). As a control to
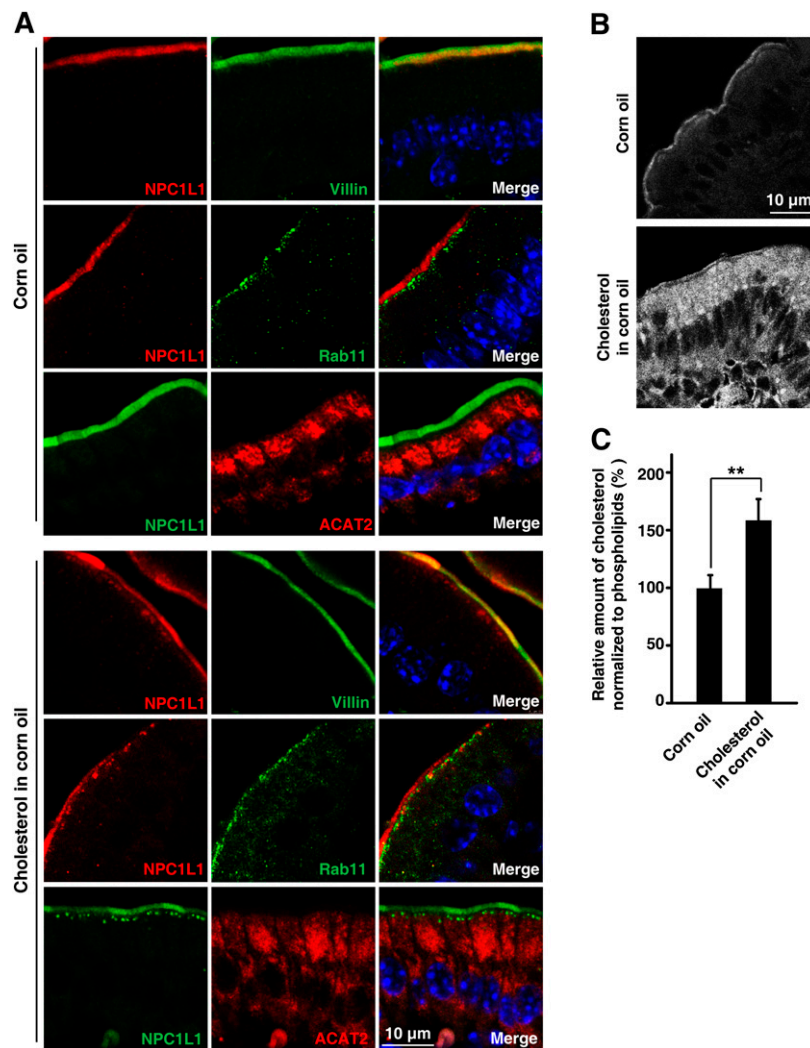
Fig. 5. Cholesterol induces endocytosis of NPC1L1 from brush border membrane toward the inside in mouse intestine. Male C57BL/6 mice (12 weeks old) were administered 200 μl corn oil or corn oil containing 40 mg/ml cholesterol by oral gavage. Thirty minutes later, proximal segments of small intestine were subjected to immunohistochemistry and filipin staining, respectively. (A) Cholesterol induced endocytosis of NPC1L1. Paraffin-embedded sections were applied to immunohistochemistry staining with anti-NPC1L1, anti-ACAT2, anti-Villin, and anti-Rab11 antibodies. Rab11 is a marker of recycling endosomes. B: Frozen sections were stained with filipin to indicate free cholesterol. C: Intestinal total cholesterol and phospholipids were measured enzymatically. The relative amount of cholesterol was normalized with that of phospholipids. Values are mean ± SD. P values were calculated by ANOVA. **$0.001 < P < 0.01$.

test the effect of ezetimibe, the cholesterol absorption in mice was measured by the fecal isotope ratio method. Ezetimibe reduced cholesterol absorption by about 80% (Fig. 6D).

Taken together, these data demonstrate that ezetimibe blocks the internalization of NPC1L1 and cholesterol in mouse small intestine.

DISCUSSION

This study illustrates that dietary cholesterol induces the endocytosis of NPC1L1 from brush border in small intestine and that ezetimibe blocks NPC1L1 and cholesterol from entering the cytoplasm. The distribution and localization of NPC1L1, ACAT2, and ACAT1 in mouse intestine were also investigated.

It has been well documented that NPC1L1 is crucial for intestinal cholesterol absorption (6, 8, 42). Most of the experiments were carried out in *NPC1L1*-null mice. Whether NPC1L1 mediates cholesterol across brush border membrane and how it functions have not been addressed in vivo. Our previous studies in cultured cells have shown that NPC1L1, together with its associated proteins Flotillin-1/-2, mediates cholesterol uptake in a vesicle-dependent manner (9, 11). Consistently, later work using small intestinal explants showed that NPC1L1 localized in the brush border in the absence of cholesterol and resided in intracellular compartments when cultured in the presence of cholesterol (43). However, ezetimibe was not investigated in that study. In addition, the experimental conditions of the cultured cells and tissues are largely different from the physiological conditions in vivo.
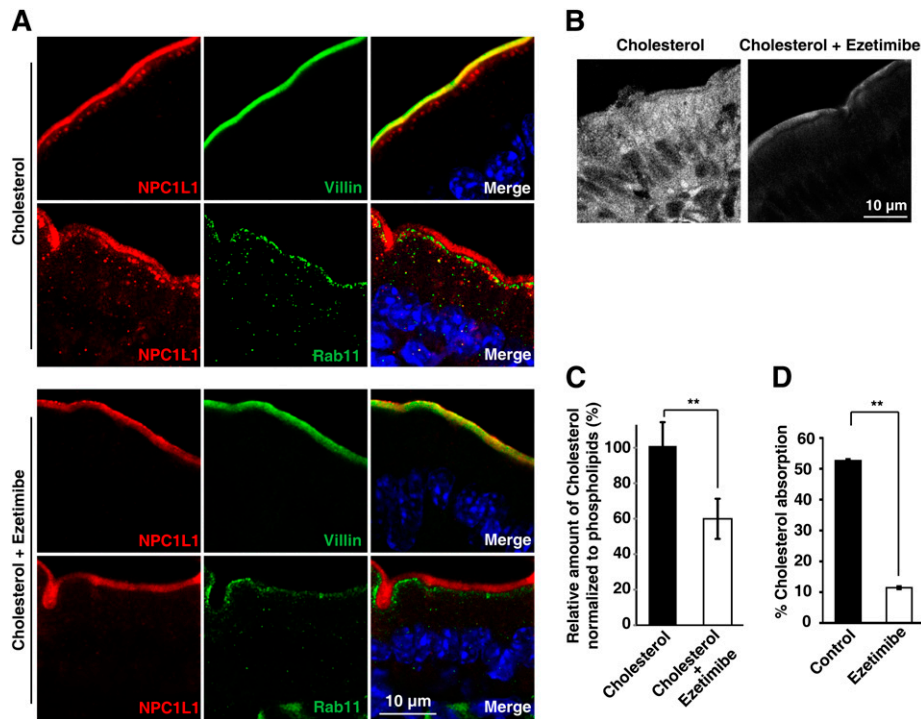
Fig. 6. Ezetimibe inhibits the internalization of NPC1L1 and cholesterol in mouse intestine. Male C57BL/6 mice (12 weeks old; n = 6 per group) were pretreated with ezetimibe or vehicle before being gavaged with cholesterol. Thirty minutes later, intestinal samples were excised and subjected to immunohistochemistry and filipin staining. A: Ezetimibe blocked cholesterol-induced endocytosis of NPC1L1. Paraffin-embedded sections were applied to immunohistochemistry staining with anti-NPC1L1 and anti-Villin or anti-Rab11 antibodies. B: Ezetimibe blocked dietary cholesterol from entering enterocytes. Frozen sections of mouse intestine were stained with filipin to indicate free cholesterol. C: Cholesterol and phospholipids were measured enzymatically. The relative amount of cholesterol was normalized to that of phospholipids. D: Male C57BL/6 mice were orally gavaged with vehicle (control) or ezetimibe once daily for 3 days. Then [^{14}C]cholesterol and [^{3}H]sitostanol in 150 µl corn oil were orally gavaged. Cholesterol absorption was determined by the fecal ratio method. Values are mean ± SD. *P* values were calculated by ANOVA. **0.001 < *P* < 0.01.

With specific antibody, we are able to show that, in the absence of intestinal luminal cholesterol, NPC1L1 mainly resides on the brush border membrane of the enterocytes and that dietary cholesterol induces the internalization of NPC1L1 to the underneath of the brush border (Figs. 1, 2, and 5). This trafficking can be impeded with the administration of ezetimibe (Fig. 6A). Ezetimibe prevents dietary cholesterol from entering cytoplasm (Fig. 6B), which causes the accumulation of cholesterol in plasma membrane (Fig. 6B).

Our study is significant because *1*) it shows for the first time that NPC1L1 functions in mediating cholesterol entering the cytoplasm of intestinal enterocytes, although previous reports that ezetimibe treatment caused upregulation of certain SREBP2 target genes implied that cholesterol was inhibited from entering the enterocytes (8, 44); *2*) dietary cholesterol induces the endocytosis of NPC1L1 from brush border; and *3*) ezetimibe blocks the internalization of NPC1L1 and cholesterol in vivo, causing their retention in plasma membrane.

Unlike what has been observed in cultured cells whose recycling endosomes were gathered into condensed complex at the perinuclear region (9, 13, 15, 16), these recycling endosomes labeled by Rab11 in intestinal tissues were localized along the brush border membrane at the subapical layer (Figs. 5A and 6A). This distinct localization of recycling endosomes may be attributed to cell polarity because Rab11 and recycling endosomes localized to subapical sites in polarized cells and tissues while being distributed to the perinuclear region in unpolarized cultured cells (12, 45, 46). The proximity between recycling endosomes and the brush border membrane probably facilitates efficient recycling of NPC1L1 and the uptake of dietary cholesterol.

Because ACAT2 but not ACAT1 was coexpressed with NPC1L1 in absorptive enterocytes (Figs. 1B, C; 2B, C; 3B, C), it implied that ACAT2 was the major enzyme for cholesterol esterification in enterocytes, consistent with previous reports (4, 20, 47–49). ACAT2 was enriched in the upper region near the brush border but had no colocalization with NPC1L1 (Figs. 2 and 5), indicating that other proteins may be required to transfer cholesterol from NPC1L1-positive endosomes to ACAT2-localized ER. More investigations are needed to identify the related factors and to illustrate the intracellular cholesterol trafficking mechanisms in small intestine.

In our study, mouse NPC1L1 is highly expressed in the jejunum and proximal ileum, which is different from the previous report that rat NPC1L1 are mainly in the duodenum and jejunum (6). The physiological conditions in the

intestinal lumen are different between mouse and rat. Mice have more hydrophilic bile acids pool (50), mainly taurocholate and tauro-β-muricholate, which are poor cholesterol solubilizers and probably lead to less efficient cholesterol absorption. As the chyme moves down, much less cholesterol is absorbed in the proximal intestine due to less efficient solubilization. High expression of NPC1L1 in jejunum and ileum would help improve the absorption efficiency. In addition, the expression of NPC1L1 in liver also shows species specificity. It is highly expressed in human but not mouse liver.

Microsomal triglyceride transfer protein (MTP) and apolipoprotein B (ApoB) play essential roles in chylomicron synthesis/assembly (51). They are also highly expressed in duodenum and jejunum but are expressed less in ileum (52). Their expression pattern is different from that of NPC1L1 and ACAT2. Because most of fatty acid was absorbed in the proximal part of the small intestine (53), the high expression of MTP and ApoB in the upper part of the intestine generates more chylomicrons to carry fatty acid and triglyceride. In the distal regions of intestine (ileum), less fatty acid is absorbed, and the relative low expression of MTP and ApoB may be enough for the incorporation of cholesterol and cholesterol ester into chylomicron. In addition, the sterol efflux transporters ATP-binding cassette transporters G5 and G8 were highly expressed in jejunum and ileum (54), similar to NPC1L1 and ACAT2, implying that the major regulation sites of cholesterol absorption may be the ileum and jejunum.

Together, these data suggest an in vivo model of dietary cholesterol absorption: The cholesterol in intestinal lumen can diffuse to the brush border membrane by bile salt micelles, and then NPC1L1 mediates cholesterol entering enterocytes via vesicular endocytosis. Cholesterol is transported to ER by unknown mechanisms and esterified by ACAT2. The cholesterol absorption inhibitor ezetimibe binds NPC1L1 (55, 56) and blocks its endocytosis, thereby preventing cholesterol from entering the cytoplasm of enterocytes.

REFERENCES

1. Wang, D. Q. 2007. Regulation of intestinal cholesterol absorption. *Annu. Rev. Physiol.* **69:** 221–248.
2. Nguyen, T. M., J. K. Sawyer, K. L. Kelley, M. A. Davis, and L. L. Rudel. 2012. Cholesterol esterification by ACAT2 is essential for efficient intestinal cholesterol absorption: evidence from thoracic lymph duct cannulation. *J. Lipid Res.* **53:** 95–104.
3. Burrier, R. E., A. A. Smith, D. G. McGregor, L. M. Hoos, D. L. Zilli, and H. R. Davis, Jr. 1995. The effect of acyl CoA: cholesterol acyltransferase inhibition on the uptake, esterification and secretion of cholesterol by the hamster small intestine. *J. Pharmacol. Exp. Ther.* **272:** 156–163.
4. Buhman, K. K., M. Accad, S. Novak, R. S. Choi, J. S. Wong, R. L. Hamilton, S. Turley, and R. V. Farese, Jr. 2000. Resistance to diet-induced hypercholesterolemia and gallstone formation in ACAT2-deficient mice. *Nat. Med.* **6:** 1341–1347.
5. Repa, J. J., K. K. Buhman, R. V. Farese, Jr., J. M. Dietschy, and S. D. Turley. 2004. ACAT2 deficiency limits cholesterol absorption in the cholesterol-fed mouse: impact on hepatic cholesterol homeostasis. *Hepatology.* **40:** 1088–1097.
6. Altmann, S. W., H. R. Davis, Jr., L. J. Zhu, X. Yao, L. M. Hoos, G. Tetzloff, S. P. Iyer, M. Maguire, A. Golovko, M. Zeng, et al. 2004. Niemann-Pick C1 Like 1 protein is critical for intestinal cholesterol absorption. *Science.* **303:** 1201–1204.
7. Davies, J. P., C. Scott, K. Oishi, A. Liapis, and Y. A. Ioannou. 2005. Inactivation of NPC1L1 causes multiple lipid transport defects and protects against diet-induced hypercholesterolemia. *J. Biol. Chem.* **280:** 12710–12720.
8. Davis, H. R., Jr., L. J. Zhu, L. M. Hoos, G. Tetzloff, M. Maguire, J. Liu, X. Yao, S. P. Iyer, M. H. Lam, E. G. Lund, et al. 2004. Niemann-Pick C1 Like 1 (NPC1L1) is the intestinal phytosterol and cholesterol transporter and a key modulator of whole-body cholesterol homeostasis. *J. Biol. Chem.* **279:** 33586–33592.
9. Ge, L., J. Wang, W. Qi, H. H. Miao, J. Cao, Y. X. Qu, B. L. Li, and B. L. Song. 2008. The cholesterol absorption inhibitor ezetimibe acts by blocking the sterol-induced internalization of NPC1L1. *Cell Metab.* **7:** 508–519.
10. Wang, L.J., and B. L. Song. 2012. Niemann–Pick C1-Like 1 and cholesterol uptake. *Biochim. Biophys. Acta.* **1821:** 964–972.
11. Ge, L., W. Qi, L. J. Wang, H. H. Miao, Y. X. Qu, B. L. Li, and B. L. Song. 2011. Flotillins play an essential role in Niemann-Pick C1-like 1-mediated cholesterol uptake. *Proc. Natl. Acad. Sci. USA.* **108:** 551–556.
12. Ullrich, O., S. Reinsch, S. Urbe, M. Zerial, and R. G. Parton. 1996. Rab11 regulates recycling through the pericentriolar recycling endosome. *J. Cell Biol.* **135:** 913–924.
13. Chu, B. B., L. Ge, C. Xie, Y. Zhao, H. H. Miao, J. Wang, B. L. Li, and B. L. Song. 2009. Requirement of myosin Vb.Rab11a.Rab11–FIP2 complex in cholesterol-regulated translocation of NPC1L1 to the cell surface. *J. Biol. Chem.* **284:** 22481–22490.
14. Hao, M., S. X. Lin, O. J. Karylowski, D. Wustner, T. E. McGraw, and F. R. Maxfield. 2002. Vesicular and non-vesicular sterol transport in living cells. The endocytic recycling compartment is a major sterol storage organelle. *J. Biol. Chem.* **277:** 609–617.
15. Xie, C., N. Li, Z. J. Chen, B. L. Li, and B. L. Song. 2011. The small GTPase Cdc42 interacts with Niemann-Pick C1-like 1 (NPC1L1) and controls its movement from endocytic recycling compartment to plasma membrane in a cholesterol-dependent manner. *J. Biol. Chem.* **286:** 35933–35942.
16. Yu, L., S. Bharadwaj, J. M. Brown, Y. Ma, W. Du, M. A. Davis, P. Michaely, P. Liu, M. C. Willingham, and L. L. Rudel. 2006. Cholesterol-regulated translocation of NPC1L1 to the cell surface facilitates free cholesterol uptake. *J. Biol. Chem.* **281:** 6616–6624.
17. Zhang, J. H., L. Ge, W. Qi, L. Zhang, H. H. Miao, B. L. Li, M. Yang, and B. L. Song. 2011. The N-terminal domain of NPC1L1 protein binds cholesterol and plays essential roles in cholesterol uptake. *J. Biol. Chem.* **286:** 25088–25097.
18. Wang, J., B. B. Chu, L. Ge, B. L. Li, Y. Yan, and B. L. Song. 2009. Membrane topology of human NPC1L1, a key protein in enterohepatic cholesterol absorption. *J. Lipid Res.* **50:** 1653–1662.
19. Uelmen, P. J., K. Oka, M. Sullivan, C. C. Chang, T. Y. Chang, and L. Chan. 1995. Tissue-specific expression and cholesterol regulation of acylcoenzyme A:cholesterol acyltransferase (ACAT) in mice. Molecular cloning of mouse ACAT cDNA, chromosomal localization, and regulation of ACAT in vivo and in vitro. *J. Biol. Chem.* **270:** 26192–26201.
20. Lee, O., C. C. Chang, W. Lee, and T. Y. Chang. 1998. Immunodepletion experiments suggest that acyl-coenzyme A:cholesterol acyltransferase-1 (ACAT-1) protein plays a major catalytic role in adult human liver, adrenal gland, macrophages, and kidney, but not in intestines. *J. Lipid Res.* **39:** 1722–1727.
21. Lee, R. G., M. C. Willingham, M. A. Davis, K. A. Skinner, and L. L. Rudel. 2000. Differential expression of ACAT1 and ACAT2 among cells within liver, intestine, kidney, and adrenal of nonhuman primates. *J. Lipid Res.* **41:** 1991–2001.
22. Chang, C. C., N. Sakashita, K. Ornvold, O. Lee, E. T. Chang, R. Dong, S. Lin, C. Y. Lee, S. C. Strom, R. Kashyap, et al. 2000. Immunological quantitation and localization of ACAT-1 and ACAT-2 in human liver and small intestine. *J. Biol. Chem.* **275:** 28083–28092.
23. Song, B. L., C. H. Wang, X. M. Yao, L. Yang, W. J. Zhang, Z. Z. Wang, X. N. Zhao, J. B. Yang, W. Qi, X. Y. Yang, et al. 2006. Human acyl-CoA:cholesterol acyltransferase 2 gene expression in

intestinal Caco-2 cells and in hepatocellular carcinoma. *Biochem. J.* **394:** 617–626.

24. Kushwaha, R. S., A. Rosillo, R. Rodriguez, and H. C. McGill, Jr. 2005. Expression levels of ACAT1 and ACAT2 genes in the liver and intestine of baboons with high and low lipemic responses to dietary lipids. *J. Nutr. Biochem.* **16:** 714–721.

25. Zhang, J., K. L. Kelley, S. M. Marshall, M. A. Davis, M. D. Wilson, J. K. Sawyer, R. V. Farese, Jr., J. M. Brown, and L. L. Rudel. 2012. Tissue-specific knockouts of ACAT2 reveal that intestinal depletion is sufficient to prevent diet-induced cholesterol accumulation in the liver and blood. *J. Lipid Res.* **53:** 1144–1152.

26. Meiner, V. L., S. Cases, H. M. Myers, E. R. Sande, S. Bellosta, M. Schambelan, R. E. Pitas, J. McGuire, J. Herz, and R. V. Farese, Jr. 1996. Disruption of the acyl-CoA:cholesterol acyltransferase gene in mice: evidence suggesting multiple cholesterol esterification enzymes in mammals. *Proc. Natl. Acad. Sci. USA.* **93:** 14041–14046.

27. Mutch, D. M., P. Anderle, M. Fiaux, R. Mansourian, K. Vidal, W. Wahli, G. Williamson, and M. A. Roberts. 2004. Regional variations in ABC transporter expression along the mouse intestinal tract. *Physiol. Genomics.* **17:** 11–20.

28. Coons, A. H., and M. H. Kaplan. 1950. Localization of antigen in tissue cells; improvements in a method for the detection of antigen by means of fluorescent antibody. *J. Exp. Med.* **91:** 1–13.

29. Sugii, S., P. C. Reid, N. Ohgami, Y. Shimada, R. A. Maue, H. Ninomiya, Y. Ohno-Iwashita, and T. Y. Chang. 2003. Biotinylated theta-toxin derivative as a probe to examine intracellular cholesterol-rich domains in normal and Niemann-Pick type C1 cells. *J. Lipid Res.* **44:** 1033–1041.

30. Borgstrom, B. 1968. Quantitative aspects of the intestinal absorption and metabolism of cholesterol and beta-sitosterol in the rat. *J. Lipid Res.* **9:** 473–481.

31. Wang, D. Q., and M. C. Carey. 2003. Measurement of intestinal cholesterol absorption by plasma and fecal dual-isotope ratio, mass balance, and lymph fistula methods in the mouse: an analysis of direct versus indirect methodologies. *J. Lipid Res.* **44:** 1042–1059.

32. Cao, J., J. Wang, W. Qi, H. H. Miao, J. Wang, L. Ge, R. A. DeBose-Boyd, J. J. Tang, B. L. Li, and B. L. Song. 2007. Ufd1 is a cofactor of gp78 and plays a key role in cholesterol metabolism by regulating the stability of HMG-CoA reductase. *Cell Metab.* **6:** 115–128.

33. Wang, L. J., J. Wang, N. Li, L. Ge, B. L. Li, and B. L. Song. 2011. Molecular characterization of the NPC1L1 variants identified from cholesterol low absorbers. *J. Biol. Chem.* **286:** 7397–7408.

34. Tang, J. J., J. G. Li, W. Qi, W. W. Qiu, P. S. Li, B. L. Li, and B. L. Song. 2011. Inhibition of SREBP by a small molecule, betulin, improves hyperlipidemia and insulin resistance and reduces atherosclerotic plaques. *Cell Metab.* **13:** 44–56.

35. Folch, J., M. Lees, and G. H. Sloane Stanley. 1957. A simple method for the isolation and purification of total lipides from animal tissues. *J. Biol. Chem.* **226:** 497–509.

36. Barker, N., J. H. van Es, J. Kuipers, P. Kujala, M. van den Born, M. Cozijnsen, A. Haegebarth, J. Korving, H. Begthel, P. J. Peters, et al. 2007. Identification of stem cells in small intestine and colon by marker gene Lgr5. *Nature.* **449:** 1003–1007.

37. Anderson, R. A., C. Joyce, M. Davis, J. W. Reagan, M. Clark, G. S. Shelness, and L. L. Rudel. 1998. Identification of a form of acyl-CoA:cholesterol acyltransferase specific to liver and intestine in nonhuman primates. *J. Biol. Chem.* **273:** 26747–26754.

38. Rudel, L. L., R. G. Lee, and T. L. Cockman. 2001. Acyl coenzyme A: cholesterol acyltransferase types 1 and 2: structure and function in atherosclerosis. *Curr. Opin. Lipidol.* **12:** 121–127.

39. Chang, T. Y., C. C. Chang, S. Lin, C. Yu, B. L. Li, and A. Miyazaki. 2001. Roles of acyl-coenzyme A:cholesterol acyltransferase-1 and -2. *Curr. Opin. Lipidol.* **12:** 289–296.

40. Chang, T. Y., B. L. Li, C. C. Chang, and Y. Urano. 2009. Acyl-coenzyme A:cholesterol acyltransferases. *Am. J. Physiol. Endocrinol. Metab.* **297:** E1–E9.

41. Temel, R. E., W. Tang, Y. Ma, L. L. Rudel, M. C. Willingham, Y. A. Ioannou, J. P. Davies, L. M. Nilsson, and L. Yu. 2007. Hepatic Niemann-Pick C1-like 1 regulates biliary cholesterol concentration and is a target of ezetimibe. *J. Clin. Invest.* **117:** 1968–1978.

42. Sane, A. T., D. Sinnett, E. Delvin, M. Bendayan, V. Marcil, D. Menard, J. F. Beaulieu, and E. Levy. 2006. Localization and role of NPC1L1 in cholesterol absorption in human intestine. *J. Lipid Res.* **47:** 2112–2120.

43. Skov, M., C. K. Tonnesen, G. H. Hansen, and E. M. Danielsen. 2011. Dietary cholesterol induces trafficking of intestinal Niemann-Pick Type C1 Like 1 from the brush border to endosomes. *Am. J. Physiol. Gastrointest. Liver Physiol.* **300:** G33–G40.

44. Telford, D. E., B. G. Sutherland, J. Y. Edwards, J. D. Andrews, P. H. Barrett, and M. W. Huff. 2007. The molecular mechanisms underlying the reduction of LDL apoB-100 by ezetimibe plus simvastatin. *J. Lipid Res.* **48:** 699–708.

45. Goldenring, J. R., J. Smith, H. D. Vaughan, P. Cameron, W. Hawkins, and J. Navarre. 1996. Rab11 is an apically located small GTP-binding protein in epithelial tissues. *Am. J. Physiol.* **270:** G515–G525.

46. Lapierre, L. A., N. A. Ducharme, K. R. Drake, J. R. Goldenring, and A. K. Kenworthy. 2012. Coordinated regulation of caveolin-1 and Rab11a in apical recycling compartments of polarized epithelial cells. *Exp. Cell Res.* **318:** 103–113.

47. Temel, R. E., R. G. Lee, K. L. Kelley, M. A. Davis, R. Shah, J. K. Sawyer, M. D. Wilson, and L. L. Rudel. 2005. Intestinal cholesterol absorption is substantially reduced in mice deficient in both ABCA1 and ACAT2. *J. Lipid Res.* **46:** 2423–2431.

48. Matsuda, H., H. Hakamata, T. Kawasaki, N. Sakashita, A. Miyazaki, K. Takahashi, M. Shichiri, and S. Horiuchi. 1998. Molecular cloning, functional expression and tissue distribution of rat acyl-coenzyme A:cholesterol acyltransferase. *Biochim. Biophys. Acta.* **1391:** 193–203.

49. Hori, M., M. Satoh, K. Furukawa, Y. Sakamoto, H. Hakamata, Y. Komohara, M. Takeya, Y. Sasaki, A. Miyazaki, and S. Horiuchi. 2004. Acyl-coenzyme A:cholesterol acyltransferase-2 (ACAT-2) is responsible for elevated intestinal ACAT activity in diabetic rats. *Arterioscler. Thromb. Vasc. Biol.* **24:** 1689–1695.

50. Wang, D. Q., and M. C. Carey. 1996. Complete mapping of crystallization pathways during cholesterol precipitation from model bile: influence of physical-chemical variables of pathophysiologic relevance and identification of a stable liquid crystalline state in cold, dilute and hydrophilic bile salt-containing systems. *J. Lipid Res.* **37:** 606–630.

51. Hussain, M. M., P. Rava, M. Walsh, M. Rana, and J. Iqbal. 2012. Multiple functions of microsomal triglyceride transfer protein. *Nutr. Metab. (Lond).* **9:** 14.

52. Swift, L. L., A. Jovanovska, B. Kakkad, and D. E. Ong. 2005. Microsomal triglyceride transfer protein expression in mouse intestine. *Histochem. Cell Biol.* **123:** 475–482.

53. Ros, E. 2000. Intestinal absorption of triglyceride and cholesterol. Dietary and pharmacological inhibition to reduce cardiovascular risk. *Atherosclerosis.* **151:** 357–379.

54. Duan, L. P., H. H. Wang, and D. Q. Wang. 2004. Cholesterol absorption is mainly regulated by the jejunal and ileal ATP-binding cassette sterol efflux transporters Abcg5 and Abcg8 in mice. *J. Lipid Res.* **45:** 1312–1323.

55. Hawes, B. E., K. A. O'neill, X. Yao, J. H. Crona, H. R. Davis, Jr., M. P. Graziano, and S. W. Altmann. 2007. In vivo responsiveness to ezetimibe correlates with niemann-pick C1 like-1 (NPC1L1) binding affinity: comparison of multiple species NPC1L1 orthologs. *Mol. Pharmacol.* **71:** 19–29.

56. Weinglass, A. B., M. Kohler, U. Schulte, J. Liu, E. O. Nketiah, A. Thomas, W. Schmalhofer, B. Williams, W. Bildl, D. R. McMasters, et al. 2008. Extracellular loop C of NPC1L1 is important for binding to ezetimibe. *Proc. Natl. Acad. Sci. USA.* **105:** 11140–11145.